PCCP

Effect of Enzymatic Orientation Through the Use of Syringaldazine Molecule on Multiple Multi-Copper Oxidase Enzymes

Journal:	*Physical Chemistry Chemical Physics*
Manuscript ID:	CP-ART-03-2014-001296.R1
Article Type:	Paper
Date Submitted by the Author:	06-May-2014
Complete List of Authors:	Ulyanova, Yevgenia; CFD Research Corporation, Babanova, Sofia; University of New Mexico, Pinchon, Erica; CFD Research Corporation, Matanovic, Ivana; University of New Mexico, Singhal, Sameer; CFD Research Corporation, Atanassov, Plamen; University of New Mexico,

Physical Chemistry Chemical Physics

Dynamic Article Links ►

Cite this: DOI: 10.1039/c0xx00000x

ARTICLE TYPE

www.rsc.org/xxxxxx

Effect of Enzymatic Orientation Through the Use of Syringaldazine Molecule on Multiple Multi-Copper Oxidase Enzymes

Yevgenia Ulyanova,[*a] Sofia Babanova,[b] Erica Pinchon,[a] Ivana Matanovic,[b] Sameer Singhal,[a] and Plamen Atanassov[b]

Received (in XXX, XXX) Xth XXXXXXXXX 20XX, Accepted Xth XXXXXXXXX 20XX
DOI: 10.1039/b000000x

The effect of proper enzyme orientation at the electrode surface was explored for two multi-copper oxygen reducing enzymes: Bilirubin Oxidase (BOx) and Laccase (Lac). Simultaneous utilization of "tethering" agent (1-pyrenebutanoic acid, succinimidyl ester; PBSE), for stable enzyme immobilization, and syringaldazine (Syr), for enzyme orientation, of both Lac and BOx led to notable enhancement of the electrodes performance. For Lac cathodes tested in solution it was established that PBSE-Lac and PBSE-Syr-Lac modified cathodes demonstrated approximately 6 and 9 times increase in current density, respectively, compared to physically adsorbed and randomly oriented Lac cathode. Further testing in solution utilizing BOx showed even higher increases in achievable current densities, thus BOx was chosen for additional testing in air-breathing mode. In subsequent air-breathing experiments the incorporation of PBSE and Syr with BOx resulted in current densities of 0.65 ± 0.1 mA/cm^2; 2.5 times higher when compared to unmodified BOx cathode. Fully tethered/oriented BOx cathode was combined with a NAD-dependent Glucose Dehydrogenase anode for the fabrication of a complete enzymatic membraneless fuel cell. Maximum power of 1.03 ± 0.06 mW/cm^2 was recorded for the complete fuel cell. The observed significant enhancement in the performance of "oriented" cathodes was a result of proper enzyme orientation, leading to facilitated enzyme/electrode interface interactions.

Introduction

The development of enzymatic biofuel cells (EFCs) has gained significant attention in recent years due to their potential use as alternative to rechargeable batteries and traditional fuel cells in the rapidly growing portable power market. EFCs possess numerous advantages over their traditional counterparts: widely available high energy density fuels; room temperature and neutral pH operating conditions; green footprint; and most importantly, the utilization of renewable bio-catalysts (enzymes) for power generation[1-3].

The level of maturity of EFCs reached the point where the rate-limiting step of their operation is the electron transfer at the enzyme-electrode interface. This imposed the development of new techniques for enzyme immobilization, such as covalent linking of the enzyme to the electrode surface or tethering through pyrene-containing compounds[4, 5]. Both of these methods proved to be successful, resulting in increased stability over short and long time periods. Another important requirement that advanced enzymatic electrodes should satisfy is the preclusion of the utilization of dissolved mediators for electron transfer, i.e. the mediator has to be co-immobilized with the enzyme or the redox enzyme has to carry out direct electron transfer (DET) from/to the solid support[5-7].

Multicopper oxidases (MCOs) such as Bilirubin Oxidase (BOx) and Laccase (Lac) have been extensively studied as catalysts for oxygen reduction reaction (ORR) due to their efficient conversion of oxygen to water[4]. The oxygen reduction to water follows a four electron transfer mechanism without the formation of toxic oxygen intermediates such as H_2O_2 and has been confirmed for both BOx and Lac[5, 7, 8]. MCOs have two substrates; the first one is the electron donor (S1) and the second one is oxygen (S2), which plays the role of electron acceptor. The T1 center of MCOs is situated close to the S1 binding pocket and is being

[a] *Y. Ulyanova, E. Pinchon, S. Singhal*
CFD Research Corporation
701 McMillian Way, Suite D
Huntsville, AL, 35806, USA
E-mail: yvu@cfdrc.com

[b] *S. Babanova, I. Matanovic, P. Atanassov*
Centennial Engineering Center, Suite 3071
University of New Mexico
1 University of New Mexico
Albuquerque, NM 87131-0001
E-mail: babanova@unm.edu

reduced during substrate oxidation. The electrons are then transferred from the T1 Cu to the trinuclear cluster (TNC), containing one T2 and two T3 Cu-atoms, and finally to S2, which, combining with protons, forms water. A unique feature of these enzymes is the ability of the T1-Cu site to accept electrons not only from enzyme's natural substrates but also from artificial electron donors, such as electrodes[5, 7]. Therefore, these enzymes can be explored for the development of enzymatic cathodes undergoing DET.

Since the T1 site of the MCOs is responsible for the electron transfer , it is essential for this site to be in close proximity to the electrode surface (d = 6.5 Å for *T. versicolor* Lac[9]). It was found that Lac-electrode interactions could be enhanced when electrode surfaces are modified with polycyclic hydrocarbons, which were supposed to penetrate the hydrophobic pocket near the T1 copper of the enzyme[10]. A hierarchically structured carbonaceous electrode matrix modified with covalently linked anthraquinone demonstrated direct electron transfer with the overall kinetics of enzymatic reaction much faster than the diffusion of dissolved oxygen[11]. The attachment of the enzyme to the electrode in study was believed to rely only on hydrophobic Lac-anthraquinone interactions. Therefore, anthraquinone and anthracene derivatives have been heavily utilized for the modification of different materials in order to facilitate the electrode-enzyme electron transfer rate[10-13].

Simplified method for electrode modification with anthracene was performed by Giroud and Minteer[14], who employed bifunctional compound with pyrene moiety for interaction with hydroxylated carbon nanotubes via π–π stacking, similarly to the interaction of the enzymatic tethers and carbon nanotubes, proposed here, and anthracene groups for enzyme attachment.

Laccases are enzymes that oxidize a range of phenolic and other organic and inorganic compounds. Since the phenol moiety-Lac recognition is based on hydrophobic interactions, the hydrophobic cleft next to the T1 site of Lac is the ideal target-binding region[10]. However, there are several other similar hydrophobic regions on the protein surface, which are not situated in the proximity of the T1 site. Attachment of the enzyme via any of these regions results in orientations of the enzyme that are unfavorable. In contrary to the concept of the hydrophobic surface-Lac interactions, Vaz-Dominguez et al. demonstrated that the presence of amino groups on the electrode surface favored DET of Lac (either adsorbed or covalently bound) and the electrode[15]. Accordingly, compounds, more specifically recognized by the enzyme, have to be explored for efficient enzyme orientation as it was previously demonstrated by our group for the orientation of BOx[16].

In contrast to fungal Lac, the residues, creating the substrate-binding pocket in BOx, are predominantly hydrophilic with the surrounding protein surface showing hydrophobic character[17]. Dos Santos et. al. observed that modification of the surface of pyrolitic graphite "edge" electrode with single aromatic ring compounds, possessing hydrophobic character, resulted in a decrease of BOx-modified electrode performance. However, when the modifiers contained carboxylic groups, an enhanced electrode performance was recorded[18]. The authors assumed that the carboxylic group located on the aromatic moiety was important for binding BOx in an orientation allowing fast electron transfer.

Both types of approaches described for the orientation of Lac and BOx rely on hydrophobic/hydrophilic interactions of the modifiers with the enzymes. For BOx, the cavity of the substrate-binding pocket is entirely internal with no openings on the surface, which assumes dynamically controlled entrance to this cavity[19] and contraries to the simple hydrophilic enzyme-substrate interactions. Therefore, our group raised the hypothesis that modification of the electrode surface with enzyme`s natural substrate will lead to recognition of the substrate by the enzyme, based on the specificity of enzyme-substrate interactions, and subsequent enzyme orientation towards the electrode surface with the substrate binding pocket facing the modified electrode[16]. Since the substrate binding pocket in MCOs is situated in the proximity of the T1 copper atom, responsible for the DET, we suggest that placing the substrate binding pocket close to the electrode surface will decrease the electron tunneling distance from the electrode to the enzyme`s T1 center and thus enhance the efficiency of the electron transfer. It was also observed by others that the potential of the T1 site appears 'tuned' for the formal reduction potential of the natural substrate of the enzyme and thus provide a driving force for the electron transfer to occur[17].

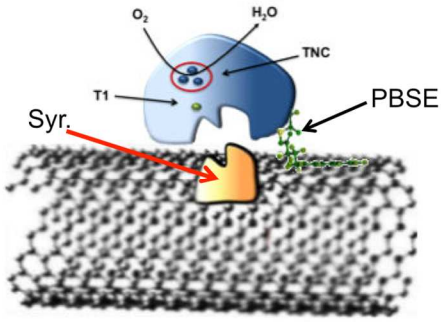

Fig. 1 Schematic representation of the concept for MCOs orientation based on the "lock and key" principle.

Here we represent the utilization of Lac natural substrate, syringaldazine (Syr), as orienting agent (OA) for two MCO enzymes: Lac and BOx. The implementation of the OA was accompanied with the utilization of tethering agent (1-pyrenebutanoic acid succinimidyl ester (PBSE)) to provide stable enzyme immobilization (Fig. **1**).

PBSE has been previously reported to link MCO to the surface of CNTs without affecting the enzyme's performance[4, 20]. The dual functionality of this tethering agent was especially beneficial; 1) the polyaromatic pyrenyl moiety would π-π stack with the surface of the nanotubes while 2) the succinimidyl moiety would covalently bind with the amino groups of the lysine residue of the protein, forming amide bonds[21]. Analogous to PBSE, Syr interacts with the carbon support through π-π stacking and, additionally, through CH- π interactions. We believe that the Syr-MCO recognition is based on the presence of protonated N-atoms, characterized with low electron density, and oxygen containing groups with high electron density, spatially separated. The presence of both of the aforementioned groups creates zwitterion, a "key" for the substrate-binding pocket, which is the "lock". More detailed computational calculations

are needed to model the Syr-MCO interactions, which are out of the scope of this study and will be performed in our future work.

Tethering and Orientation of Laccase

Spatially orienting the enzyme at the electrode surface can potentially decrease the distance between the electrode and the enzyme active center and therefore increase the rate of ORR and the overall achievable current density of the cathode[10]. It was hypothesized that the presence of enzyme`s natural substrate at the electrode surface would enhance the favorable positioning of the active center of the protein towards the surface of the electrode. Lac from *T. versicolor*, a relatively well-studied oxygen-reducing enzyme, was integrated with multi-walled nanotubes (MWNTs) to fabricate enzymatic ink, further employed in the development of air-breathing cathodes. Syringaldazine, Lac natural substrate, which is often used to detect the presence and investigate the activity of Lac[22-26], was used as OA. The crystallographic structure of *T. versicolor* Lac shows that the T1 site is surrounded by a negatively charged pocket, due to carboxylic residues that are non-protonated at pH values above 4–5[9]. Therefore it was supposed that some of the Syr-Lac interactions are provided through the negatively charged carboxylic groups of the enzyme and the positively charged moieties of Syr. In order to determine the surface charge distribution of Syr, electrostatic potential of Syr was calculated on the b3lyp/6-31+G(d,p) level of theory and mapped onto the electron density surface at the contour of 0.002 au (Figure 2). Since the pK_a value of Syr is 8.2[27], at pHs 6 and 7.5, the pHs of the current study, the N-atoms in Syr are protonated. Although the molecule of Syr is electroneutral as a whole it has spatially separated charges. When protonated, the surface at the proximity of the N-atoms is characterized with low electron density, while the surface close to the O-atoms (from the oxygen containing groups) is characterized with high electron density (Fig. **2**). The presence of both charges creates zwitterion, which is recognized by the substrate-binding pocket.

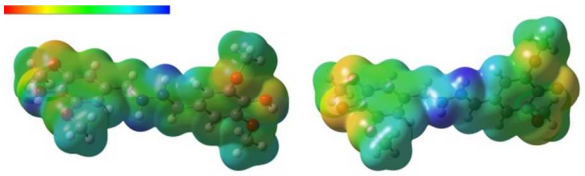

Fig. 2 Electrostatic potential of syringaldazine mapped onto the electron density surface at a contour of 0.002 au, calculated at b3lyp/6-31+G(d,p) level of theory. Left) reduced form, right) oxidized form. The values on the scale vary from -0.18*e* to 0.18*e* , red indicates negative electrostatic potential and blue is a positive potential.

In addition, the nature of Syr-carbon support interactions was investigated using computational methods (Fig. 3 Syringaldazine adsorbed on graphene sheet obtained using density functional theory with vdW-DF functional The optimized geometry of Syr, adsorbed on graphene sheet, was obtained using generalized gradient approximation (GGA) to density functional theory (DFT) with vdW-DF functional proposed by Dion et al.[28, 29] and projector augmented-wave pseudopotential[30, 31] as implemented in Vienna Ab initio Software Package (VASP)[32-35]. It was established that graphene sheet interacts with Syr through Van der Waals forces; π-π interactions are most dominant with the ring parallel to the surface and CH-π interactions with the ring placed almost orthogonal to the sheet (83°). The absorption energy was determined to be -1.70 eV.

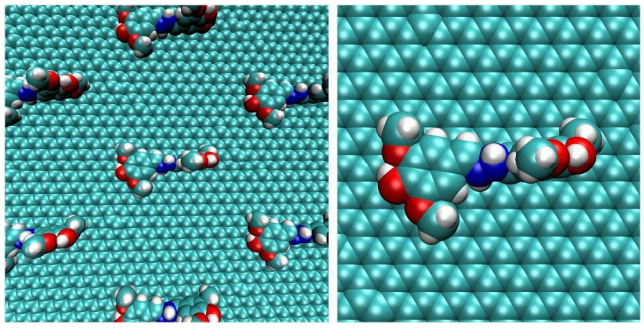

Fig. 3 Syringaldazine adsorbed on graphene sheet obtained using density functional theory with vdW-DF functional.

Five carbon nanotube composites were prepared and studied. The first four included a suspension of MWNTs, Lac, and either Syr or PBSE, or Syr and PBSE simultaneously: MWNTs-Lac, MWNTs-Syr-Lac, MWNTs-PBSE-Lac and MWNTs-Syr-PBSE-Lac[36]. The last composite, MWNTs-Syr, contained only MWNTs suspension and Syr and was utilized as a non-enzymatic control to determine the onset of the potential wave due to the electrochemical activity of Syr. All initial testing was performed on modified glassy carbon Rotating Disk Electrode (RDE) in solution. Linear voltammetry (LV) plots of the four enzyme/nanotubes composites clearly showed the wave due to oxygen reduction (Fig. **4**). The onset potential of the oxygen reduction in the presence of Syr as OA was slightly higher than in the other cases. The maximum reduction current recorded increased in the following order: MWNTs-Lac; MWNTs-Syr; MWNTs-Syr-Lac; MWNTs-PBSE-Lac; MWNTs-Syr-PBSE-Lac. The oxidation and reduction peaks, between 125 and 350 mV, were due to the electrochemical transformation of Syr itself. This compound possesses electrochemical activity as evident from the CVs of Syr in solution and adsorbed onto nanotubes (data not shown). Current values were taken at 0.4 V vs. sat. Ag/AgCl, prior to the onset of the Syr reduction, and compared over the four Lac/MWNTs composite type electrodes tested. The oxygen reduction current observed in the presence of Syr was 2.3 times higher than the ORR on MWNTs without any tethering and orienting agents. When Syr was incorporated with PBSE and Lac, the observed current densities were 16 times higher than for the physically adsorbed Lac (MWNTs-Lac). It should also be noted that the slope of the reduction wave was steeper for oriented/tethered enzymatic electrodes as compared to other types of enzyme immobilization.

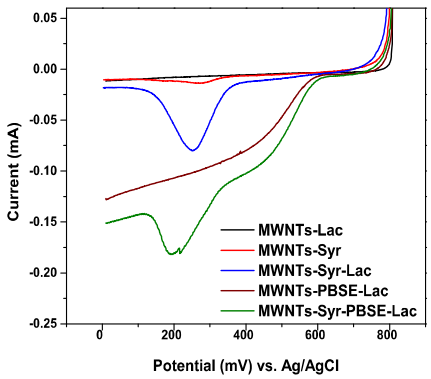

Fig. 4 Representative linear voltammograms for the five composites: MWNT-Lac, MWNT-Syr, MWNTs-Syr-Lac, MWNT-PBSE-Lac and MWNT-Syr-PBSE-Lac. Experiments were performed in oxygen saturated 0.1M phosphate buffer (pH 6) at 1600 rpm at a scan rate of 10 mV/s.

The observed trend suggested that when an orienting agent was used, the catalytic efficiency increased significantly, enhancing the kinetics of the oxygen reduction. Due to the electrochemical activity of Syr we further supposed that this compound not only provides advanced enzyme orientation but also participates in the electron transfer [37]. The functionality of Syr as a mediator was investigated for Syr modified carbon ceramic electrode and silicate encapsulated Lac[38], resulting in the absence of DET from Lac due to hindered interaction of the enzyme with the electrode surface. An increase in the cathodic peak of Syr was observed in the presence of Lac and oxygen, indicating enzymatic ORR. The onset potential of the cathodic wave of the Syr-Lac electrode corresponded to the onset potential of Syr reduction, demonstrating purely mediator function of Syr.

In the present study the function of Syr is primarily of an OA, as evident from Fig. **4**. The onset potential of the ORR coincides with the redox potential of Lac T1 center.

A comparison of the current densities from potentiostatic polarization curves is shown in Fig. **5**. Since the current response of the control samples (MWNTs-Syr and MWNTs-Syr-Lac) was notably smaller than MWNTs-PBSE-Lac and MWNTs-Syr-PBSE-Lac they were not included in the polarization study.

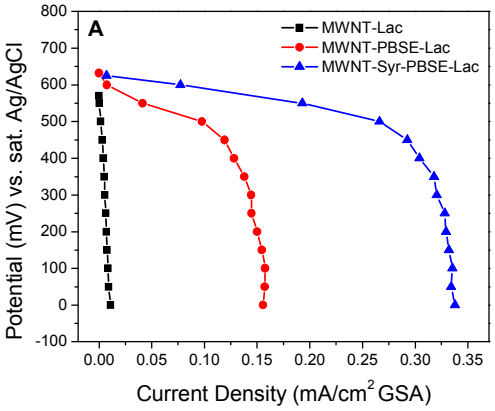

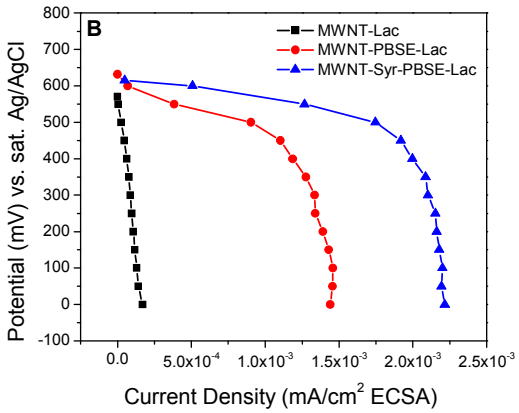

Fig. 5 Representative potentiostatic polarization curves of the Lac/MWNTs composites: (A) normalized to the geometric surface area of RDE; (B) normalized to the electrochemically accessible surface area of the nanotube composite. Experiments were performed in 0.1M phosphate buffer (pH 6).

The results, normalized to either geometric surface area (GSA) or electrochemical accessible surface area (ECSA) of the MWNTs composites, revealed that Syr was responsible for the significant increase in the observed current densities due to specific spatial enzyme orientation. The current density generated at 0.3 V vs. sat. Ag/AgCl from the electrode containing only Lac was 0.006 ± 0.005 mA/cm^2 (GSA), the current density for the PBSE tethered enzyme was 0.144 ± 0.013 mA/cm^2 (GSA), and the current density in the presence of OA (Syr) as well as PBSE was 0.320 ± 0.022 mA/cm^2 (GSA). The polarization experiments of the electrode with PBSE and Syr demonstrated more than two times increase in the maximum current densities compared to PBSE-Lac only cathode.

The effectiveness of Syr as orienting agent for Lac was confirmed by determining the so-called "orienting efficiency" of the implied organic substance. The orienting efficiency was calculated by dividing the current recorded when direct electron transfer is applied by the enzyme in presence of OA, and the current generated when a mediator is introduced into the system:

$$OE = \frac{DET\ current}{MET\ current} * 100 \qquad \text{Eq. 1}$$

2,2'-azino-bis(3-ethylbenzothiazoline-6-sulphonic acid) (ABTS) was explored as a mediator. Since ABTS is able to diffuse and exchange electrons between the electrode and the T1 site of immobilized enzyme molecules, the rate of MET should be independent of the orientation of the later and should be representative for the amount of active Lac placed on the electrode surface. At the same time, only the immobilized Lac molecules that have a redox site close to the electrode surface should participate in DET and generate current.

The electrode composite MWNTs-Syr-PBSE-Lac was polarized with constant potential of 0.3 V vs. sat. Ag/AgCl and the corresponding current was recorded (Fig. **6**). Once the current stabilized, an aliquot of ABTS solution (ABTS + $e^- \rightarrow ABTS^{\cdot-}$ with $E^{\circ\prime} = 0.883$ V vs. sat. Ag/AgCl) was added and the resulting current was monitored as a function of time. Using Eq. 1, it was established that the orienting efficiency of Syr was 55 ± 4 %. This result is in perfect agreement with previously published observations for aminophenyl and 2-aminophenol modified

electrodes utilizing covalently bonded *T. hirsuta* Lac (55% and 43% OE respectively at pH 4.2)[15].

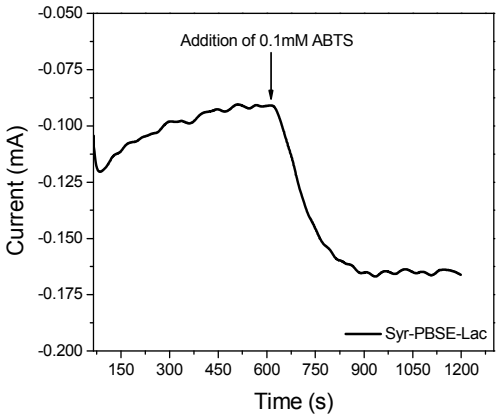

Fig. 6 Representative chronoamperometric curve (0.3 V vs. sat. Ag/AgCl) for MWNTs-Syr-PBSE-Lac cathode: prior and post the addition of ABTS as mediator.

Tethering and Orientation of Bilirubin Oxidase

Electrochemical testing of oriented enzyme nanocomposite electrodes in solution

As an alternative to Lac the use of BOx was investigated. BOx, an oxygen-reducing enzyme widely used for the design of air-breathing cathodes in EFCs, is capable of undergoing DET at the electrode surface [6]. BOx's natural substrate is Bilirubin (Biru), however, BOx can also oxidase several other organic compounds such as Catechol and Syr, which could potentially be utilized as alternatives to very costly Biru. Syr was chosen as orienting agent for direct comparison with Lac. The assumption that the enzyme-Syr interactions are based on "charge recognition" is even more reliable for BOx since its substrate binding pocket is hydrophilic[19].

Initial testing of the electrochemical activity of the enzyme was performed utilizing RDE in solution as for Lac. LVs were carried out in phosphate buffer solution (0.1 M, pH 7.5), followed by potentiostatic polarization measurements. Sample electrodes were prepared utilizing both PBSE and Syr (MWNTs-Syr-PBSE-BOx). For comparison purposes, LV of a control electrode (MWNTs-PBSE-BOx), without the use of the OA was also performed. It can be seen that the limiting current observed with fully oriented/tethered electrode was practically identical to that obtained with tethered-only electrodes when results were normalized to the GSA (Fig. **7**). However, when results were normalized to the ECSA, eliminating the variation in electrode surface (amount of nanotube/enzyme mixture dropped on the electrode surface), the limiting current for fully oriented/tethered electrodes became more pronounced (Fig. **7**, insert). It is known that the electrode behavior is determined by the amount and the orientation of the enzyme. The current, generated at high potentials, was identical for both sample and control electrodes, indicating that the enzyme amount was the same. However, at lower potentials, the current was significantly higher for Syr-oriented electrode (normalized to ECSA) but still lower than BiRu-oriented BOx electrodes[16]. The latter indicates more efficient orientation of the enzyme when its natural substrate is used. Further optimization of Syr system could yield results close to Biru system.

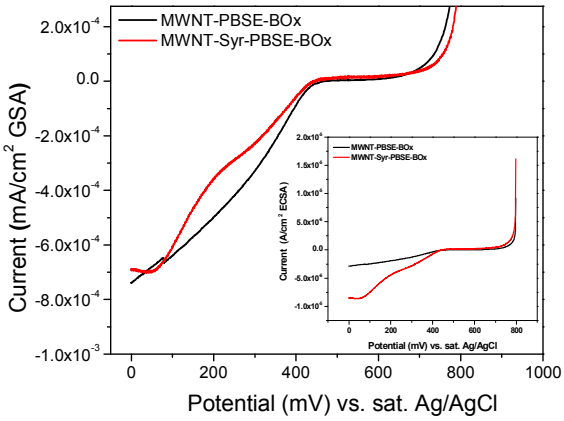

Fig. 7 Representative linear voltammograms of BOx/MWNTs composites; insert shows results normalized to the electrochemical accessible surface area. Experiments were performed in 0.1M phosphate buffer (pH 7.5).

As with Lac, the orienting efficiency of BiRu towards BOx orientation was examined. Biru was utilized in order to determine the maximum orienting efficiency that could be achieved for BOx. The chronoamperoemtric curve for MWNTs-Biru-PBSE-BOx electrode is depicted in Fig. **8**. The calculated orienting efficiency, based on Eq. 1, was 97 ± 6% when BOx's natural substrate was utilized as orienting agent. In comparison, it has been shown that BOx orienting efficiency can reach 90 % when orienting agent, other than the natural substrate, is employed [16].

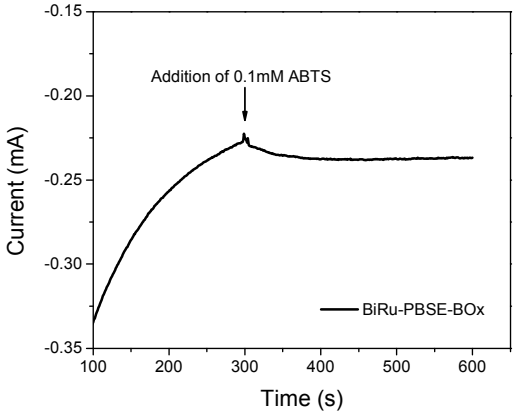

Fig. 8 Representative chronoamperometric curve (0.3 V vs. Ag/AgCl) for MWNTs-Biru-PBSE-BOx cathode: prior and post the addition of ABTS mediator.

BOx was down selected as the most promising MCO enzyme, based on its higher orienting efficiency in presence of BiRu and more favourable operational pH, (pH of 7.5 is closer to that of the intended anodic enzymes), and was therefore employed in the development of an air-breathing electrode as described in the section below.

Electrochemical testing of oriented enzyme nanocomposite electrodes in air-breathing mode

Further testing was performed utilizing air-breathing composite electrodes in order to maximize the available oxygen concentration. There are several factors that must be taken into account in addition to enzyme orientation. One such factor is the stability of enzyme immobilization at the electrode surface since the overall cathodic performance depends on the enzyme amount present. If the concentration of the enzyme at the electrode surface decreases with time, the electrode performance will also decrease. Therefore, the choice of enzyme immobilization technique is critical in attaining high electrochemical performance. Usually, BOx is physically adsorbed at the electrode surface. However, such immobilization technique results in relatively poor enzyme retention, leading to a decrease in current density as the enzyme desorbs from the electrode with time. In order to improve enzyme retention and thus achievable current density, BOx was attached to the electrode surface through the use of a tethering agent, PBSE.

Two gas-diffusion BOx cathodes were fabricated. The first one had physically adsorbed BOx and the second one explored enzyme tethering through PBSE. When the electrodes were tested immediately after preparation, the polarization curves were similar for physically adsorbed and tethered cathodes with higher current densities recorded at high potentials with the tethered BOx (Fig. **9**). The lack of significant differences in performance of the two types of immobilized cathodes suggests that tethering of the enzyme had no adverse effect on the overall catalytic activity of BOx. However, when the cathodes were allowed to sit in a constant contact with the electrolyte for 24 hours after preparation, there was significant variation in the generated current densities between tethered and adsorbed electrodes. Current density for physically adsorbed electrode after 24 hours was 1.75 times lower than for the same electrode tested immediately after fabrication. This decrease in performance can be attributed to a decrease in the enzyme concentration at the electrode surface, as portion of the deposited enzyme had desorbed. For tethered BOx electrode a performance decrease of about 10 % was observed, which is the range of the relative standard deviation of the preparation of the air breathing cathodes and the measurement procedure as a whole (RSD < 20% for physically adsorbed samples and RSD < 10 % for PBSE tethered samples). Thus, in order to have relatively stable performance over prolonged period of time, tethering of the enzyme with PBSE was chosen as an immobilization technique for all further cathode designs..

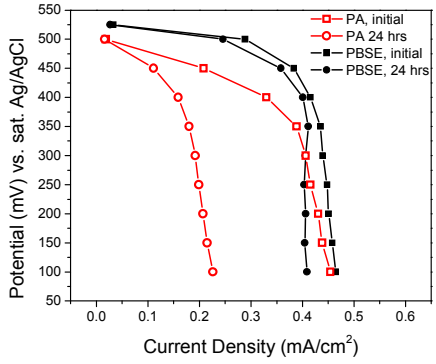

Fig. 9 Representative polarization curves for MWNT-BOx-modified air-breathing cathodes: physical adsorption (PA) vs. tethering (PBSE). Experiments were performed in phosphate buffer (pH 7.5)

A number of cathodes were tested in order to determine the effect of OA, TA and the combination of the two on the overall electrode performance in air-breathing mode. It was not only important to study the effects of the OA and TA, but also determine the optimal concentrations of the two agents for highest achievable electrode performance. As previously mentioned, the current density depends on the amount of the enzyme present at the cathode. If the concentration of the TA is too low, not all available enzymes can be tethered to the electrode surface, resulting in a decrease in the current density. The same can be said for the OA concentration. It was determined through potentiostatic polarization measurements that doubling the concentrations of OA and TA, based on enzyme concentration, was sufficient to achieve highly stable enzyme loading at the electrode surface with adequate enzyme orientation (Fig. **10**).

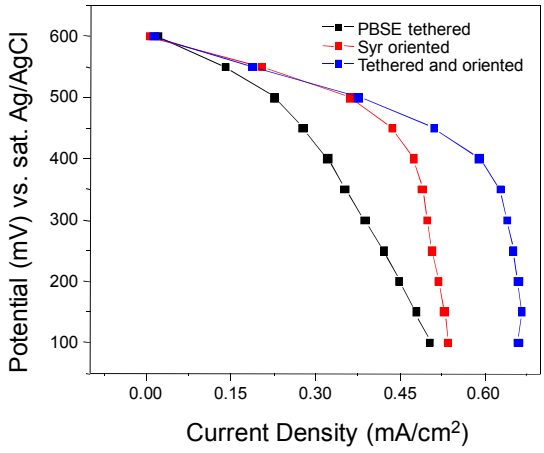

Fig. 10 Representative polarization curves for MWNTs-BOx modified cathodes: tethered (PBSE), oriented (Syr), and tethered/oriented (PBSE/Syr). Experiments were performed in phosphate buffer (pH 7.5).

Complete Enzymatic Fuel Cell Testing

Based on the individual enzyme experiments it was determined that the performance of BOx in the presence of OA/TA was significantly higher than that of Lac. For this purpose BOx modified cathode was chosen to be tested in a full EFC set-up. Complete EFC testing was performed in a membraneless single chamber fuel cell, employing Glucose Dehydrogenase (GDH) anode and BOx air-breathing cathode. The GDH anode was composed of a single-walled carbon nanotube ink with cross-linked GDH and deposited on polymethylene green (PMG) modified MWNTs paper. The BOx air-breathing cathode incorporated tethering and orienting agents simultaneously, as previously described. In order to maximize oxygen concentration, eliminating diffusional limitations, the outer side of the cathode was exposed to forced oxygen (an excess of oxygen) during the test. The electrolyte solution consisted of 1 M glucose/10 mM NAD^+ in 0.245 M sodium phosphate buffer (pH 7). Constant load discharge (CLD) technique was performed where a series of resistances were applied to the cell and the potential and current were monitored as a function of time. Results for EFC testing for both randomly oriented but tethered cathode (MWNTs-PBSE-BOx) and an oriented and tethered cathode (MWNTs-PBSE-Syr-BOx) are depicted in Fig. **11**. The current and power densities are reported as a function of GSA.

The carried out measurements demonstrate a 2.5 times increase in overall fuel cell performance using the oriented cathode developed in this study. Furthermore, the individual polarization curves confirm that the improvement comes from the cathode side of the EFC. The recorded maximum power of 1.03 ± 0.06 mW/cm^2 is one of the highest power density reported for glucose-based membraneless EFC.

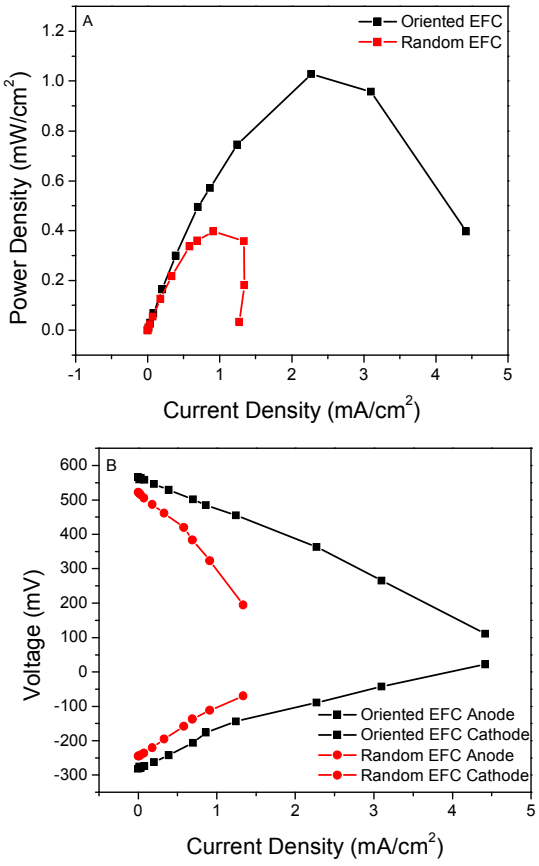

Fig. 11 (A) Power and (B) individual polarization curves for complete enzymatic fuel cell demonstrating 2.5 times increase in power for the oriented nanocomposite electrode. Experiments were performed in phosphate buffer (pH 7).

Conclusions

The concept of utilizing Syringaldazine, Laccase`s natural substrate, as orienting agent in combination with a tethering agent, for efficient enzyme immobilization, was successfully proven for both BOx and Lac-based composite electrodes. The improvement in the modified cathodes performance was most likely due to enhanced interfacial electron transfer as a result of more favorable T1-Cu site orientation towards the electrode surface. When Syr was incorporated with PBSE and Lac, the observed ORR current densities were 1.3 times higher in comparison to PBSE-only modified electrodes and 16 times higher than for physically adsorbed cathodes. Significant enhancement of the achievable current and power densities was observed when a modified gas-diffusion BOx cathode was designed and integrated into a complete enzymatic fuel cell. EFC`s current densities were 3 times higher when BOx was preferentially oriented as compared to random enzyme orientation. Maximum power of 1.03 ± 0.06 mW/cm^2 was reported for the complete EFC.

The employment of a single orienting agent across multiple MCOs enzymes shows a path forward for the development of highly efficient air-breathing cathodes and their utilization in the design of enzymatic fuel cells.

Notes and references

Electrochemical cathode testing in solution

A 1 wt% MWNTs (cheaptubes.com, d = 20 - 30 nm, L = 10 – 30 μm) ink solution containing 0.1 wt% tetrabutylammonium bromide modified Nafion (TBAB-Nafion) (in ethanol/water mixture) was prepared following previously described procedure[16]. Syringaldazine was dissolved in ethanol and then added to the MWNTs/TBAB-Nafion suspension to a final concentration of 10 mM. Once the orienting agent was added, the ink suspension was incubated for 1 hour prior to addition of PBSE and the enzyme. Stock enzyme solutions (Lac from *Trameters hirsute* (EC 1.10.3.2.), Sigma Aldrich; BOx from *Myrothecium verrucaria* (EC 1.3.3.5.), Amano Enzyme U.S.A. Co., Ltd.) were prepared in 0.1 M phosphate buffer (pH 6 and pH 7.5, respectively). PBSE (in ethanol) and stock enzyme solution were added to MWNT ink in a final concentration of 10 mM and 10 mg/mL, respectively. A 10 μL aliquot of the final ink suspension was deposited onto glassy carbon rotating disc electrode (RDE, GSA=0.2475 cm^2) and allowed to dry prior testing. Before ink deposition of each sample, the RDE was cleaned with alumina slurry with increasing fine grits of 1 μm, 0.3 μm, and 0.05 μm, rinsing with DI water between polishings.

The RDE measurements of the ink composites were performed in a three-electrode set up with RDE used as working electrode, Pt wire counter and sat. Ag/AgCl as reference electrodes. 0.1 M potassium phosphate buffer (pH 7.5 for BOx studies and pH 6 for Lac) was utilized as electrolyte. LVs, CVs, and potentiostatic polarization curve data was collected on a 16 channel potentiostat (VMP3, Bio-logic, USA LLC). LV and CV working electrode potential was swept from a +0.8 V to 0.0 V at a scan rate of 10 mV/s. Rotation rates for LV experiments were varied from 0 RPM to 1600 RPM in 400 RPM intervals. The potentiostatic polarization curves were carried out by chronoamperometric measurements of 300 seconds starting from an open circuit potential (OCP) of the electrode and decreasing to 0 V at 50 mV intervals. The chronoamperometry steps for the potentiostatic polarization curves were performed without rotation of the working electrode.

Electrochemical cathode testing in air-breathing mode

Composite air-breathing cathodes were fabricated by employing teflonized carbon black powder (35% teflonization, XC35), Toray paper (Fuel Cell Store) and commercially available high conductivity MWNTs paper (Buckeye Composites). The XC35 was sandwiched between the perforated Toray paper and the MWNTs paper and hydraulically pressed for 5 minutes at 500 psi[39]. A 100 μL volume of the MWNTs ink (as described earlier) was deposited onto the MWNTs paper (2.85 cm^2) and allowed to dry. Potentiostatic polarization curves were carried out as previously described using VMP3 potentiostat. Pt wire was used

as counter electrode. The applied potentials were measured versus sat. Ag/AgCl reference electrode.

Complete fuel cell testing

Glucose Dehydrogenase (GDH (EC 1.1.99.10) from Amano Enzyme USA) anodes were prepared as follows: polymethylene green (PMG) was electrodeposited onto MWNTs paper (Buckeye Composites) from a methylene green (MG) monomer solution (0.5mM MG in 50 mM potassium phosphate buffer, pH 7, with 0.1 M potassium nitrate) by cycling the potential from 1.3 to -0.5 V vs. sat. Ag/AgCl at a scan rate of 5 mV/s for 10 cycles[40]. After PMG deposition, the electrodes were thoroughly washed with deionized water to remove any unreacted methylene green and dried under ambient conditions. Once dry, the electrodes were modified with patented SWNTs ink[41] containing 1 mg/cm^2 GHD. The nanotube ink was prepared by suspending SWNTs (99% purity, Cheaptubes.com) in an aqueous solution of polyethyleneimine (PEI) (medium MW, Sigma-Aldrich), dissolved in 50 mM sodium phosphate buffer (pH 7). 5.7 mg of GDH was dissolved in 200 µL of the SWNT ink. 6.9 mg of both 1-ethyl-3-(3-dimethylaminopropyl)carbodiimide hydrochloride (EDC) and N-hydroxysuccinimide (NHS) were added to the ink. Finally, 100 µL of the ink was deposited onto the PMG modified MWNTs paper (2.85 cm^2 geometric surface area) and incubated at 4 °C overnight prior to testing.

BOx gas-diffusion cathodes were prepared as previously described. MWNTs/TBAB-Nafion ink with PBSE, Syr, and BOx was deposited onto the electrode surface and allowed to dry under ambient conditions. GDH-modified anode and BOx-modified cathode were placed in polycarbonate hardware. Electrolyte solution consisted of 1 M glucose/10 mM NAD^+ in 0.245 M sodium phosphate buffer (pH 7). The outer side of the cathode was exposed to forced oxygen. Constant load discharge (CLD) technique was employed for fuel cell testing where a series of resistances (from 5 MΩ to 5 Ω) were applied to the cell while current and voltage were monitored as a function of time. Individual electrode polarization curves as well as full cell power curves were generated for the membraneless fuel cell.

All electrochemical studies were performed under ambient laboratory conditions.

Computational Calculations

The electrostatic potential of Syr at the isodensity surface of 0.002 au was calculated based on density functional theory with b3lyp functional and 6-31+G(d,p) basis set using Gaussian 09 quantum chemical software package[42]. Geometries were optimized in water using polarizable continuum model.

Optimized geometry of Syr, adsorbed on the graphene sheet, was obtained using generalized gradient approximation (GGA) to density functional theory (DFT) with the vdW-DF functional proposed by Dion et al.[28, 29] and projector augmented-wave pseudopotential[30, 31] as implemented in Vienna Ab initio Software Package (VASP)[32-35]. Graphene sheet was represented by (6x6) supercell with dimensions of 25.56 Å x 25.56 Å and vacuum region of 15 Å. Electronic energy was calculated using 5x5x1 k-point Monkhorts-Pack mesh[43] and tetrahedron method with Blöchl corrections. Plane-wave basis cutoff was set to 400 eV. The adsorption energy was calculated as:

$$\Delta E_{ad} = E_{surface+ad} - [E_{surface} + E_{ad}] \quad \text{Eq. 2}$$

where E_{ad} is the energy of an isolated molecule. In order to analyze the interaction between Syr and the support we compared the total density of states of bare and Syr-adsorbed surface.

1. W. Gellett, M. Kesmez, J. Schumacher, N. Akers and S. D. Minteer, *Electroanalysis*, 2010, **22**, 727-731.
2. G. P. M. K. Ciniciato, C. Lau, A. Cochrane, S. S. Sibbett, E. R. Gonzalez and P. Atanassov, *Electrochimica Acta*, 2012, **82**, 208-213.
3. S. Calabrese Barton, J. Gallaway and P. Atanassov, *Chemical Reviews*, 2004, **104**, 4867-4861-4886.
4. R. P. Ramasamy, H. R. Luckarift, D. M. Ivnitski, P. B. Atanassov and G. R. Johnson, *Chemical Communications*, 2010, **46**, 6045.
5. S. Brocato, C. Lau and P. Atanassov, *Electrochimica Acta*, 2012, **61**, 44-49.
6. G. Gupta, Lau, C., Branch, B., Rajendran, V., Ivnitski, D., Atanassov, P., *Electrochimica Acta*, 2011, **56**, 10767-10771.
7. S. Shleev, G. Shumakovich, O. Morozova and A. Yaropolov, *Fuel Cells*, 2010, **10**, 726-733.
8. M. C. Weigel, E. Tritscher and F. Lisdat, *Electrochemistry Communications*, 2007, **9**, 689-693.
9. K. Piontek, M. Antorini and T. Choinowski, *The Journal of Biological Chemistry*, 2002, **277**, 37663–37669.
10. C. F. Blanford, R. S. Heath and F. A. Armstrong, *Chem. Commun.*, 2007, 1710–1712.
11. M. Sosna, L. Stoica, E. Wright, J. D. Kilburn, W. Schuhmann and P. N. Bartlett, *Phys. Chem. Chem. Phys., 2012*, 2012, **14**, 11882–11885.
12. M. Sosna, J.-M. Chretien, J. D. Kilburn and P. N. Bartlett, *Physical Chemistry Chemical Physics*, 2010, **12**, 10018–10026.
13. M. S. Thorum, C. A. Anderson, J. J. Hatch, A. S. Campbell, N. M. Marshall, S. C. Zimmerman, Y. Lu and A. A. Gewirth, *J Phys Chem Lett.* , 2010, **11**, 2251–2254.
14. F. Giroud and S. D. Minteer, *Electrochemistry Communications*, 2013, **34**, 157-160.
15. C. Vaz-Dominguez, S. Campuzano, O. Rudiger, M. Pita, M. Gorbacheva, S. Shleev, V. M. Fernandez and A. L. D. Lacey, *Biosensors and Bioelectronics* 2008, **24**, 531–537.
16. R. J. Lopez, S. Babanova, Y. Ulyanova, S. Singhal and P. Atanassov, *ChemElectroChem*, 2014, **1**, 241-248.
17. J. A. Cracknell, T. P. McNamara, E. D. Lowe and C. F. Blanford, *Dalton Trans.*, 2011, **40**, 6668-6675.
18. L. dos Santos, V. Climent, C. F. Blanford and F. A. Armstrong, *Phys. Chem. Chem. Phys.,*, 2012, **12**, 13962–13974.
19. J. A. Cracknell, T. P. McNamara, E. D. Lowe and C. F. Blanford, *Dalton Transitions*, 2011, **40**, 6668-6675.
20. L. Halámková, J. Halámek, V. Bocharova, A. Szczupak, L. Alfonta and E. Katz, *Journal of the American Chemical Society*, 2012, **134**, 5040-5043.
21. R. J. Chen, Y. Zhang, D. Wang and H. Dai, *J. Am. Chem. Soc*, 2001, **123**, 3838-3839.
22. J. M. Harkin, M. J. Larsen and J. R. Obst, *Mycologia*, 1974, **66**, 469-476.
23. J. M. Harkin and J. R. Obst, *Experientia*, 1973, **29**, 381-508.
24. A. Leonowicz and K. Grzywnowicz, *Enzyme Microb. Technol*, 1981, **2**, 55-58.
25. M. C. Machczynski, E. Vijgenboom, B. Samyn and G. W. Canters, *Protein Science*, 2004, **13**, 2388-2397.
26. J. Rotková, R. Šuláková, L. Korecká, P. Zdražilová, M. Jandová, J. Lenfeld, D. Horák and Z. Bílková, *Journal of Magnetism and Magnetic Materials*, 2009, **321**, 1335-1340.
27. F. Xu, *The Journal of Biological Chemisry*, 1997, **272**, 924–928.
28. M. Dion, H. Rydberg, E. Schröder, D. C. Langreth and B. I. Lundqvist, *Physical review letters*, 2004, **92**.

29. J. Klimeš, D. R. Bowler and A. Michaelides, *Journal of Physics: Condensed Matter*, 2010, **22**, 022201.
30. P. E. Blöchl, *Physical Review B*, 1994, **50**, 17953-17979.
31. G. Kresse and D. Joubert, *Physical Review B*, 1999, **59**, 1758-1775.
32. G. Kresse and J. Hafner, *Physical Review B*, 1993, **47**, 558-561.
33. G. Kresse and J. Hafner, *Physical Review B*, 1994, **49**, 14251-14269.
34. G. Kresse and J. Furthmüller, *Computational Materials Science*, 1996, **6**, 15-50.
35. G. Kresse and J. Furthmüller, *Physical Review B*, 1996, **54**, 11169-11186.
36. N. S. Parimi, Y. Umasankar, P. Atanassov and R. P. Ramasamy, *ACS Catalysis*, 2012, **2**, 38-44.
37. C. Fernandez-Sanchez, T. Tzanov, G. M. Gubitz and A. Cavaco-Paulo, *Bioelectrochemistry*, 2002, **59**, 149– 156.
38. W. Nogala, E. Rozniecka, J. Rogalski and M. Opallo, *Journal of Electroanalytical Chemistry* 2007, **608**, 31-36.
39. S. Babanova, K. Artyushkova, Y. Ulyanova, S. Singhal and P. Atanassov, *Journal of Power Sources*, 2014, **245**, 389-397.
40. C. W. Narváez Villarrubia, R. A. Rincón, V. K. Radhakrishnan, V. Davis and P. Atanassov, *ACS Applied Materials & Interfaces*, 2011, **3**, 2402-2409.
41. V. Svoboda, J. Wei and S. Singhal, *US Patents 8,685,286 and 8,703,022*, 2014.
42. M. J. Frisch, *Gaussian 09, Revision C.01*, (2010), Inc., Wallingford CT.
43. H. J. Monkhorst and J. D. Pack, *Physical Review B*, 1976, **13**, 5188-5192.